

Published in final edited form as:

Curr Biol. 2008 February 12; 18(3): 177–182. doi:10.1016/j.cub.2007.12.050.

STIM1 is a microtubule plus end tracking protein involved in remodeling of the endoplasmic reticulum

Ilya Grigoriev^{1,*}, Susana Montenegro Gouveia^{1,*}, Babet van der Vaart¹, Jeroen Demmers², Jeremy T. Smyth³, Srinivas Honnappa⁴, Daniël Splinter¹, Michel O. Steinmetz⁴, James W. Putney Jr³, Casper C. Hoogenraad⁵, and Anna Akhmanova^{1,#}

¹ Department of Cell Biology, Erasmus Medical Center, 3000 CA Rotterdam, The Netherlands ² Department of Biochemistry, Erasmus Medical Center, 3000 CA Rotterdam, The Netherlands ³ Laboratory of Signal Transduction, National Institute of Environmental Health Sciences NIH, Department of Health and Human Services, USA ⁴ Biomolecular Research, Structural Biology, Paul Scherrer Institut, CH-5232 Villigen PSI, Switzerland ⁵ Department of Neuroscience, Erasmus Medical Center, 3000 CA Rotterdam, The Netherlands

Abstract

Stromal interaction molecule 1 (STIM1) is a transmembrane protein that is essential for store-operated Ca²⁺ entry, a process of extracellular Ca²⁺ influx in response to the depletion of Ca²⁺ stores in the endoplasmic reticulum (ER) (reviewed in [1–4]). STIM1 localizes predominantly to the ER; upon Ca²⁺ release from the ER, STIM1 translocates to the ER-plasma membrane junctions and activates Ca²⁺ channels (reviewed in [1–4]). Here we show that STIM1 directly binds to the microtubule plus end tracking protein EB1 and forms EB1-dependent comet-like accumulations at the sites where polymerizing microtubule ends come in contact with the ER network. Therefore, the previously observed tubulovesicular motility of GFP-STIM1 [5] is not a motor-based movement but a traveling wave of diffusion-dependent STIM1 concentration in the ER membrane. STIM1 overexpression strongly stimulates ER extension occurring through the microtubule “tip attachment complex” (TAC) mechanism [6,7], a process whereby an ER tubule attaches to and elongates together with the EB1-positive end of a growing microtubule. Depletion of STIM1 and EB1 decreases TAC-dependent ER protrusion, indicating that microtubule growth-dependent concentration of STIM1 in the ER membrane plays a role in ER remodeling.

Keywords

store operated calcium entry; microtubule dynamics; endoplasmic reticulum; STIM1; EB1

Results and Discussion

STIM1 binds directly to EB1

We used the fact that the majority of microtubule (MT) plus end tracking proteins (+TIPs) directly bind to EB1 or its homologues (reviewed in [8]) to identify novel +TIPs. We performed glutathione S-transferase (GST) pull down assays with cell extracts using GST-EB1, EB2 and EB3 fusions and analyzed the isolated proteins by mass spectrometry. Among the proteins which were highly enriched in the GST-EB pull downs but did not bind to GST alone we found

#Correspondence should be addressed to: Dr. Anna Akhmanova, Dept. Cell Biology, Erasmus Medical Center, P.O. Box 2040, 3000 CA Rotterdam, The Netherlands. Tel: +31-10-4638134, Fax: +31-10-4089468, e-mail: a.akhmanova@erasmusmc.nl.

*These authors contributed equally to this manuscript.

many known +TIPs (Table S1, [8]). One of the most abundant potential new partners of EB1 and EB3 was STIM1; its homologue STIM2 was also present in the GST-EB1/EB3 pull-downs (Table S1). The association of STIM1 with the EB family members was specific: while GFP alone did not interact with any GST fusions, GFP-STIM1 strongly associated with GST-EB1 and GST-EB1 C-terminus but not with GST alone or with GST-EB1 N-terminus (Fig. 1A). Compared to GST-EB1, GFP-STIM1 showed reduced binding to GST-EB3 and GST-EB2, in line with the mass spectrometry data (Table S1). The interaction between EB1 and STIM1 is direct, because purified EB1 bound to the purified GST fusion of STIM1 C-terminus (Fig. 1B,G). The fact that EB1 and STIM1 associate with each other under physiological conditions was confirmed by co-immunoprecipitation of endogenous proteins (Fig. 1E).

GFP-STIM1, expressed in HeLa cells at low levels, localized in an ER-like pattern, as shown before [5,9] (Fig. 1C). Within this pattern we observed comet-like structures that coincided with some of the MT ends positive for the endogenous EB1 (Fig. 1C). This explains the previously described partial colocalization of GFP-STIM1 with microtubules [5,10].

STIM1 is a multidomain transmembrane protein, with the N-terminus located in the ER lumen and the C-terminus in the cytoplasm (Fig. 1G) (reviewed in [11]). By expressing GFP-fused deletion mutants of STIM1, we mapped the minimal domain of STIM1 required for MT plus end association to a part of the C-terminus including a portion of the ezrin-radixin-moesin (ERM) domain and the basic serine-proline (S/P) rich region (fragment STIM1-C3, amino acids 392–652) (Fig. 1D,G). This fragment was efficiently pulled down by GST-EB1 and EB1-C-terminus, similar to the full length STIM1 (Fig. 1F). It is likely that the positively charged S/P-rich region of STIM1 is involved in binding to EB1, because similar domains of other +TIPs also perform this function [12].

STIM1 associates with growing MT ends—Using live cell imaging we observed that in HeLa cells GFP-STIM1 highlighted the ER network through which comet-like structures traveled with an average velocity of $0.22 \pm 0.07 \mu\text{m/s}$ (mean \pm SD, calculated from 5 cells) (Video 1). These comets coincided with growing MT ends visualized with EB3-mRFP, a MT plus end marker [13] (Fig. S1A,B, Video 2). Comet-like behavior of GFP-STIM1 was also observed in MRC5-SV fibroblasts, which have a sparse MT array and are therefore better suited for distinguishing individual ER tubules and MT tips. Also in these cells GFP-STIM1 localized to the ER (visualized with a luminal ER marker) and mobile comets within the ER network (Fig. 2A, Video 3). In addition, we also observed immobile accumulations of GFP-STIM1, which likely represented an overexpression artifact in this cell type (Video 3,4). All GFP-STIM1 comets coincided with EB3-mRFP-positive MT ends (Fig. 2B, C, Video 4). When a growing MT tip arrived at the edge of the ER network, an ER tubule with a STIM1-positive accumulation at its tip often extended together with the growing MT. When the connection between the MT end and the ER tubule was lost, the ER tubule retracted while the MT end usually continued growing (Fig. 2C). Once a growing MT end came in contact with another ER tubule, STIM1 accumulation at the MT tip reappeared. This dynamic behavior explains why only some of the EB1/EB3-labeled MT ends are GFP-STIM1 positive: GFP-STIM1 comets are only present at the sites of physical contact between MT ends and ER membranes.

These observations were confirmed by simultaneous imaging of GFP-STIM1 and MTs (Fig. 2D, Fig. S2, Video 5). Accumulations of GFP-STIM1 were detected only at the ends of growing, but not shortening or pausing MTs (Fig. 2D, Fig. S2). Again we observed simultaneous extension of MTs and ER tubules with GFP-STIM1 comets at their tips; these comets were lost either after the MT underwent a catastrophe (Fig. S2) or because the ER tubule lost connection with the MT end (Fig. 2D). MT polymerization-dependent ER tubule extension was described previously in *Xenopus* extracts and in newt lung epithelial cells; this type of ER

tubule formation was named “tip attachment complex” (TAC) mechanism, as opposed to ER sliding along preexisting MTs [6,7].

The fact that GFP-STIM1 comets disappeared once the contact between MT tips and the ER was lost and reappeared soon after this contact was re-established, suggested that individual GFP-STIM1 molecules do not undergo processive MT-based transport. Analysis of GFP-STIM1 fluorescence recovery after photobleaching (FRAP) showed that GFP-STIM1 diffuses in the ER slower than EB3-mRFP in the cytoplasm (Fig. 3A,B). Recovery of the diffuse GFP-STIM1 signal in the ER network in the bleached region always preceded the appearance of MT tip-associated GFP-STIM1 comets (Fig. 3A), supporting the idea that GFP-STIM1 molecules arrive at the growing MT end by diffusion. Therefore, the observed “movement” of GFP-STIM1 comets actually represents a traveling wave of GFP-STIM1 concentration at the sites of EB1-positive MT end - ER membrane interaction.

Ca²⁺ release from the ER abolishes STIM1 plus end tracking behavior—Previous studies showed that when Ca²⁺ stores in the ER are depleted by the addition of thapsigargin, STIM1 oligomerized and redistributed to peripheral foci [2–4,11,14]. Indeed, thapsigargin treatment caused rapid relocalization of GFP-STIM1 into immobile ER-associated puncta (Video 6). FRAP experiments showed, in line with previous publications [14], that the exchange of GFP-STIM1 in thapsigargin-induced foci was strongly diminished (Fig. 3B). In MRC5-SV fibroblasts, the dynamics of EB-positive MT ends was not significantly affected by thapsigargin and EB1/EB3 were only weakly associated with the immobile GFP-STIM1 (Fig. 3C, Video 7 and data not shown). In contrast, in HeLa cells a proportion of the endogenous and overexpressed EB proteins still displayed colocalization with the immobile GFP-STIM1 accumulations (Fig. S3 and data not shown); FRAP assay showed that EB3-mRFP underwent rapid exchange at these sites (Fig. 3B). The difference between the two cell types might be due to the differential expression of additional EB and/or STIM1-binding partners. These data suggest that STIM1 oligomerization after Ca²⁺ release from the ER does not preclude its association with the EBs. However, in the oligomerized state, STIM1 diffuses within the ER much more slowly ([14], Fig. 3B) and as a result it can no longer track growing MT tips (Fig. 3C, Video 7).

Comet-like behavior of STIM1 depends on EB1 and is not essential for store-operated Ca²⁺ entry (SOCE)—EB1 is the predominant EB species in HeLa cells (Akhmanova, unpublished data) and its knockdown was sufficient to significantly reduce the accumulation of other +TIPs at the MT ends [15]. GFP-STIM1 still showed ER-like distribution after EB1 depletion, but its accumulation in mobile comets was abolished (Fig. 4A,B, Fig. S1C, Video 8 and data not shown) indicating that it is EB1-dependent. Also blocking MT dynamics by the addition of nocodazole or taxol, which abolish MT end accumulation of the mammalian +TIPs [13,16], completely abrogated the comet-like localization of GFP-STIM1 (Fig. 4C, Fig. S1D, E).

GFP-STIM1 puncta induced by Ca²⁺ release still formed in EB1-depleted cells (data not shown); moreover, EB1 knockdown or the inhibition of MT dynamics by taxol had no significant influence on thapsigargin-induced SOCE in HeLa cells, whereas STIM1 siRNA transfection had a significant inhibitory effect (Fig. S4). Therefore, it appears that MT growth-dependent concentration of STIM1 is not necessary for STIM1-mediated activation of SOCE when intracellular Ca²⁺ stores are depleted with thapsigargin.

STIM1 and EB1 are required for TAC-mediated ER tubule extension—Observation of the ER dynamics using luminal ER markers together with MTs showed that TAC-mediated tubule formation does occur in MRC5-SV cells but is rare compared to sliding of new ER tubules along preexisting MTs (Table S2). TAC-associated and sliding events occurred with

clearly different velocities: MT-tip attached ER tubules grew at $\sim 0.2 \mu\text{m/s}$, which corresponds to the MT growth rate in these cells, while ER sliding occurred with velocities up to $\sim 5 \mu\text{m/s}$. Remarkably, in GFP-STIM1-expressing cells the frequency of TAC-driven ER tubule formation events increased ~ 12 fold (Table S2).

Since TAC-mediated ER protrusion events are infrequent in MRC5-SV fibroblasts, these cells are not a convenient model to study the TAC mechanism. We therefore turned to HeLa cells where TAC-mediated tubule formation constitutes $\sim 21\%$ of all ER tubule extension events (among 18.5 ± 6.7 new ER tubule formation events detected per $200 \mu\text{m}^2$ per 1 min, 3.9 ± 2.2 were TAC-mediated; $n=20$ cells; Fig. 4D,E, Video 9). We inhibited the expression of EB1 and STIM1 by siRNA transfection and found that while the knockdown of either protein had no effect on the expression of the other (Fig. 4A), individual depletion of each protein reduced the frequency of TAC-dependent ER protrusions without significantly affecting the number of sliding events or the MT density (Fig. 4D,E, Fig. S5). In contrast, the expression of GFP-STIM1 increased the number of TAC-mediated events; this effect was not observed in EB1-depleted cells, indicating that it is EB1-dependent (Fig. 4D). It appears, therefore, that STIM1 in the ER membrane and EB1 at the growing MT tip participate in forming the molecular link responsible for MT polymerization-dependent ER tubule extension. It should be noted that the suppression of TAC-dependent ER protrusion by STIM1 and EB1 depletion was not complete; the residual events can be explained by the incomplete knockdown of the two proteins and by the potential participation of their homologues, STIM2 and EB3, in ER protrusion.

Interestingly, both in MRC5-SV and HeLa cells the frequency of ER tubule sliding was reduced after GFP-STIM1 expression, while sliding velocity was not affected (Table S2, Fig. 4E). GFP-STIM1 expression did not suppress ER tubule sliding in EB1-depleted cells, where no upregulation of TAC-driven ER protrusion was observed; as a result, in all conditions tested the total number of ER tubule formation events remained relatively constant (Fig. S5A), suggesting that it may depend on some intrinsic properties of the ER network.

Conclusions—We have identified STIM1 as a MT plus end binding protein. Its dynamics is similar to those of other mammalian +TIPs: it is based on diffusion combined with transient accumulation at the freshly polymerized MT end. However, in contrast to all other known +TIPs, STIM1 is diffusing not in the cytoplasm but in the ER membrane. Our data show that a MT tip growing along a membrane can continuously remodel it by concentrating certain molecules for which it has affinity. Furthermore, our findings suggest that a specific interaction of membrane-embedded molecules with the growing MT ends can create forces that are sufficient to cause membrane deformation and tubule extension, similar to motor-based pulling of membrane tubules along stabilized MTs [17].

While a recent study showed that complete MT depolymerization affects Ca^{2+} release-activated Ca^{2+} currents [10], our experiments failed to find an effect of MT stabilization or EB1 depletion on SOCE, indicating that comet-like behavior of STIM1 plays no significant role in regulating Ca^{2+} influx when Ca^{2+} stores are fully depleted by thapsigargin treatment. Still, it is possible that in physiological conditions MT growth-dependent ER-remodeling and STIM1 concentration could be important for the formation of ER-plasma membrane junctions and the spatial organization of Ca^{2+} signaling.

Supplementary Material

Refer to Web version on PubMed Central for supplementary material.

Acknowledgements

We thank K. Bezstarosti and P. Wulf for technical assistance. We are grateful to R. Tsien and R. Lewis for the gift of materials. This work was supported by the Netherlands Organization for Scientific Research grants 814.02.005 and 816.02.016 to A.A., by the Dutch Ministry of Economic Affairs (BSIK), by Fundação para a Ciência e a Tecnologia fellowship to S.G., by the Netherlands Organization for Scientific Research (NWO-ZonMw-VIDI), the European Science Foundation (European Young Investigators (EURYI)) awards to C.C.H, by the Swiss National Science Foundation through Grant 3100A0-109423 to M.O.S. and by the Intramural Research Program of the NIH, National Institute of Environmental Health Sciences (J.T.S and J.W.P.).

References

1. Luik RM, Lewis RS. New insights into the molecular mechanisms of store-operated Ca²⁺ signaling in T cells. *Trends Mol Med* 2007;13:103–107. [PubMed: 17267286]
2. Putney JW Jr. New molecular players in capacitative Ca²⁺ entry. *J Cell Sci* 2007;120:1959–1965. [PubMed: 17478524]
3. Hogan PG, Rao A. Dissecting ICRAC, a store-operated calcium current. *Trends Biochem Sci* 2007;32:235–245. [PubMed: 17434311]
4. Wu MM, Luik RM, Lewis RS. Some assembly required: Constructing the elementary units of store-operated Ca(2+) entry. *Cell Calcium*. 2007
5. Baba Y, Hayashi K, Fujii Y, Mizushima A, Watarai H, Wakamori M, Numaga T, Mori Y, Iino M, Hikida M, Kurosaki T. Coupling of STIM1 to store-operated Ca²⁺ entry through its constitutive and inducible movement in the endoplasmic reticulum. *Proc Natl Acad Sci U S A* 2006;103:16704–16709. [PubMed: 17075073]
6. Waterman-Storer CM, Salmon ED. Endoplasmic reticulum membrane tubules are distributed by microtubules in living cells using three distinct mechanisms. *Curr Biol* 1998;8:798–806. [PubMed: 9663388]
7. Waterman-Storer CM, Gregory J, Parsons SF, Salmon ED. Membrane/microtubule tip attachment complexes (TACs) allow the assembly dynamics of plus ends to push and pull membranes into tubulovesicular networks in interphase *Xenopus* egg extracts. *J Cell Biol* 1995;130:1161–1169. [PubMed: 7657700]
8. Lansbergen G, Akhmanova A. Microtubule plus end: a hub of cellular activities. *Traffic* 2006;7:499–507. [PubMed: 16643273]
9. Wu MM, Buchanan J, Luik RM, Lewis RS. Ca²⁺ store depletion causes STIM1 to accumulate in ER regions closely associated with the plasma membrane. *J Cell Biol* 2006;174:803–813. [PubMed: 16966422]
10. Smyth JT, Dehaven WI, Bird GS, Putney JW Jr. Role of the microtubule cytoskeleton in the function of the store-operated Ca²⁺ channel activator STIM1. *J Cell Sci* 2007;120:3762–3771. [PubMed: 17925382]
11. Dziadek MA, Johnstone LS. Biochemical properties and cellular localisation of STIM proteins. *Cell Calcium*. 2007
12. Galjart N. CLIPs and CLASPs and cellular dynamics. *Nat Rev Mol Cell Biol* 2005;6:487–498. [PubMed: 15928712]
13. Stepanova T, Slemmer J, Hoogenraad CC, Lansbergen G, Dortland B, De Zeeuw CI, Grosveld F, van Cappellen G, Akhmanova A, Galjart N. Visualization of microtubule growth in cultured neurons via the use of EB3-GFP (end-binding protein 3-green fluorescent protein). *J Neurosci* 2003;23:2655–2664. [PubMed: 12684451]
14. Liou J, Fivaz M, Inoue T, Meyer T. Live-cell imaging reveals sequential oligomerization and local plasma membrane targeting of stromal interaction molecule 1 after Ca²⁺ store depletion. *Proc Natl Acad Sci U S A* 2007;104:9301–9306. [PubMed: 17517596]
15. Watson P, Stephens DJ. Microtubule plus-end loading of p150(Glued) is mediated by EB1 and CLIP-170 but is not required for intracellular membrane traffic in mammalian cells. *J Cell Sci* 2006;119:2758–2767. [PubMed: 16772339]
16. Perez F, Diamantopoulos GS, Stalder R, Kreis TE. CLIP-170 highlights growing microtubule ends in vivo. *Cell* 1999;96:517–527. [PubMed: 10052454]

17. Koster G, VanDuijn M, Hofs B, Dogterom M. Membrane tube formation from giant vesicles by dynamic association of motor proteins. *Proc Natl Acad Sci U S A* 2003;100:15583–15588. [PubMed: 14663143]

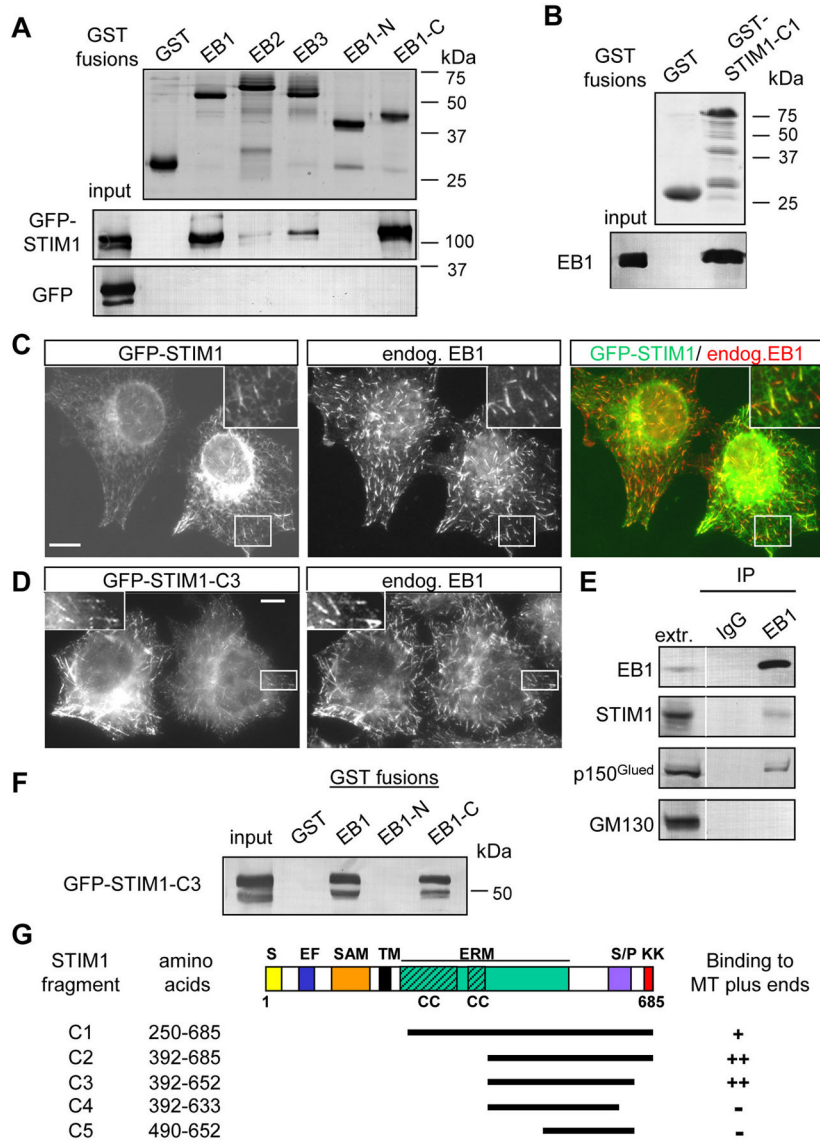


Figure 1. STIM1 interacts with EB1

A,B,F. GST pull down assays with the indicated GST fusions; extracts of HEK293 cells overexpressing GFP-STIM1, GFP-STIM1-C3 mutant or GFP alone were used in **A** and **F**, and the purified full length EB1 protein in **B**. Coomassie-stained gels are shown for GST fusions; other proteins were detected by Western blotting with antibodies against GFP (**A**, **F**) or EB1 (**B**).

C, D. HeLa cells were transfected with GFP-STIM1 or GFP-STIM1-C3 mutant, fixed and stained for the endogenous EB1. The insets show enlargements of the boxed areas. In the overlay GFP-STIM1 is shown in green and EB1 in red. Bars, 10 μ m.

E. Immunoprecipitation from extracts of HeLa cells with the rabbit polyclonal antibody against EB1 or a control rabbit serum. The lane marked “extr.” shows 5% of the input. Dynactin subunit p150^{Glued}, a known EB1 partner, was used as a positive control, and GM130, a protein associated with the cytoplasmic side of the Golgi, as a negative control.

G. Mapping of the minimal MT plus end binding domain of STIM1 by colocalization with EB1 in fixed HeLa cells. A scheme of STIM1 protein structure and the deletion mutants is shown; S, signal peptide; EF, EF hand; SAM, sterile α motif domain; TM, transmembrane

domain; ERM, ezrin-radixin-moesin domain; CC, coiled coil; S/P, serine-proline rich domain; KK, lysine-rich domain.

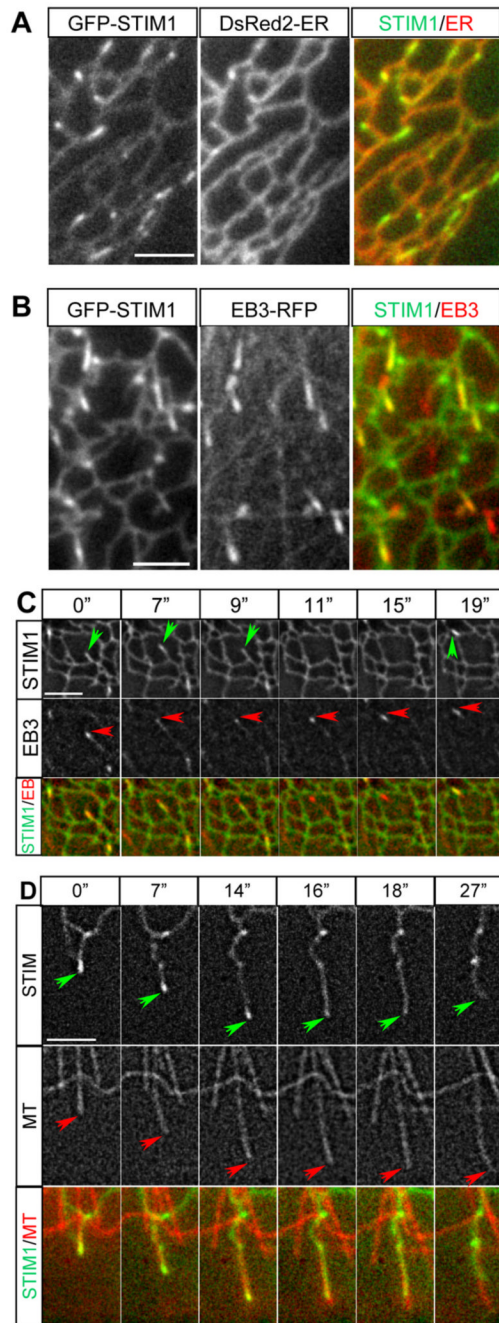


Figure 2. GFP-STIM1 colocalizes with ER and MT plus ends in live cells

A. Simultaneous imaging of GFP-STIM1 (green in overlay) and DsRed2-ER (red in overlay) in a transiently transfected MRC5-SV cell.

B,C. Simultaneous imaging of GFP-STIM1 (green in overlay) and EB3-mRFP (red in overlay) in a transiently transfected MRC5-SV cell; a single frame is shown in **B**; successive frames from Video 4 are shown in **C** (time is indicated above the panels). GFP-STIM1 comets are indicated by green arrows and EB3-mRFP comets are highlighted by red arrows.

D. Simultaneous imaging of GFP-STIM1 (green in overlay) and mCherry- α -tubulin (red in overlay) in a transiently transfected MRC5-SV cell. Successive frames are shown; time is

indicated above the panels. Tips of extending/retracting ER tubules and MTs are indicated by green and red arrows, respectively. Bars, 3 μm .

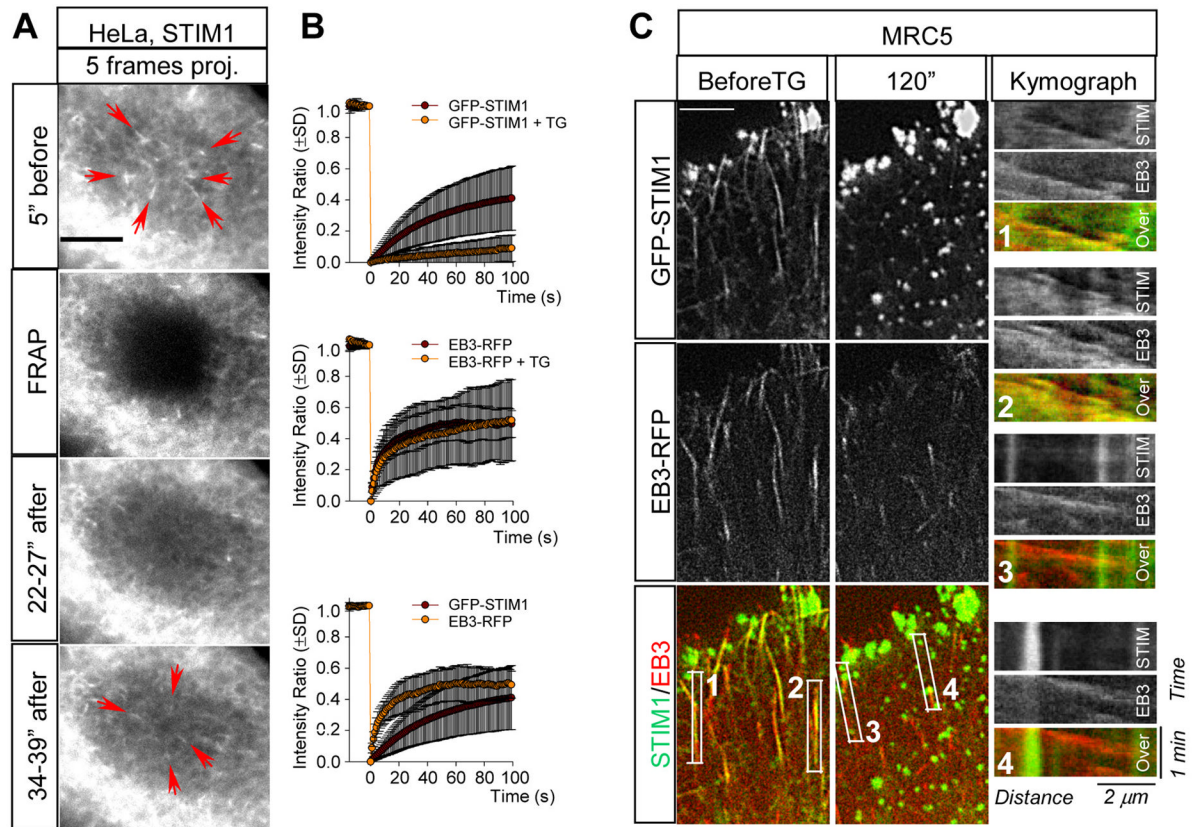


Figure 3. Analysis of GFP-STIM1 dynamics in control cells and after Ca^{2+} store depletion

A. FRAP analysis of GFP-STIM1 behavior. Each panel, with the exception of the panel marked "FRAP" (which shows a single frame), represents superimposition of 5 successive frames with a 1s interval. Note that recovery of diffuse ER signal in the bleached area precedes the appearance of GFP-STIM1 comets (indicated by red arrows).

B. The average GFP-STIM1 intensity ratio of two regions inside and outside of the photobleached area in HeLa cells (measured as described in [14]). Left: control cells, $n = 20$; cells after addition of $2 \mu\text{M}$ thapsigargin (TG), $n = 13$ cells; middle: control cells, $n = 7$; $2 \mu\text{M}$ thapsigargin $n = 12$ cells; right: GFP-STIM1, $n = 20$ cells; EB3-mRFP, $n = 7$ cells.

C. Representative frames of simultaneous two-color video of an MRC5-SV cell expressing GFP-STIM1 and EB3-RFP before and 120s after the addition of $2 \mu\text{M}$ thapsigargin in normal culture medium. Kymographs illustrating the changes of fluorescent intensity over time in the indicated boxed areas are shown on the right. In kymographs motile comets appear as slopes and immobile structures as vertical lines. Bars, $5 \mu\text{m}$.

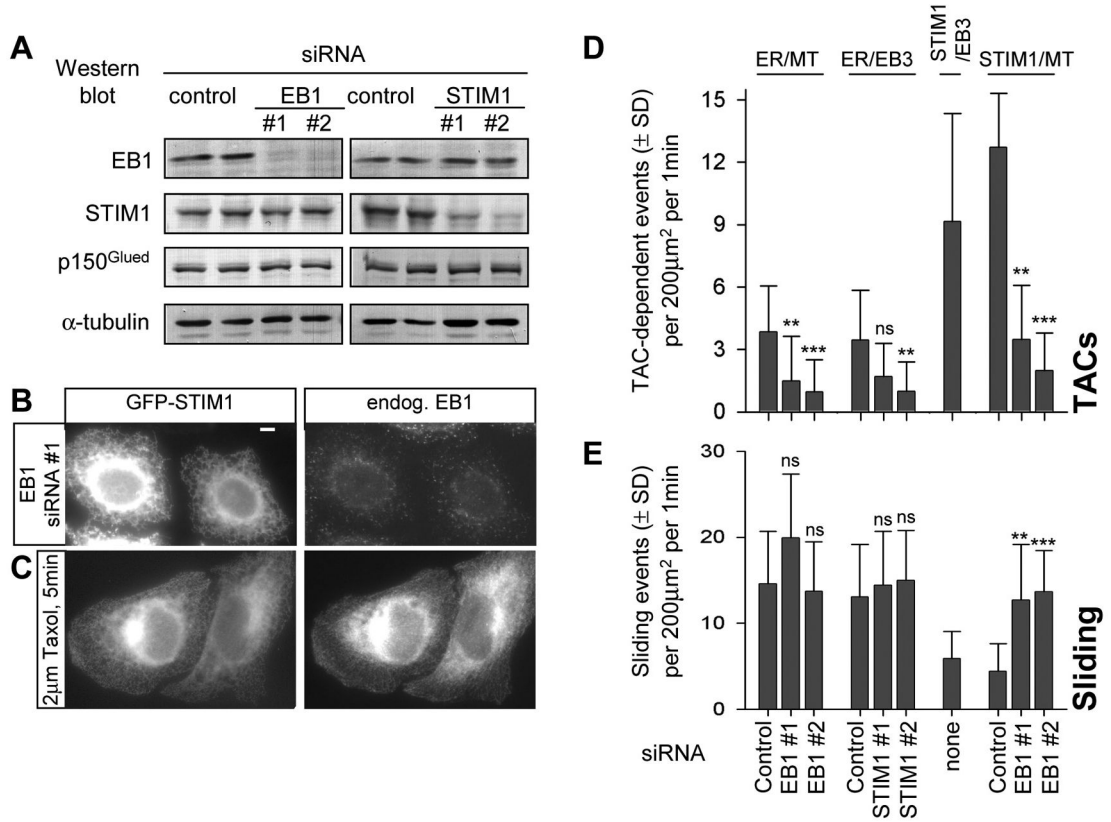


Figure 4. EB1 and STIM1 are required for TAC-mediated ER extension

A. Western blot analysis of extracts of HeLa cells 3 days after transfection with the indicated siRNAs.

B. HeLa cells were transfected with the siRNA EB1#1; two days later the cells were transfected with GFP-STIM1, cultured for one more day, fixed and stained for EB1. Bar, 5 μ m.

C. HeLa cells transfected with GFP-STIM1 were treated with taxol, fixed and stained for EB1.

D, E. HeLa cells were transfected with the indicated siRNAs; one day later cells were transfected with plasmid DNA, cultured for two more days and used for dual color imaging. The following combinations of fluorescent markers were used: mCherry- α -tubulin (stably expressed in HeLa cells) together with transiently expressed YFP-ER; transiently expressed EB3-mRFP and YFP-ER, transiently expressed EB3-mRFP and GFP-STIM1; mCherry- α -tubulin (stably expressed in HeLa cells) together with transiently expressed GFP-STIM1.

D. Number of TACs, determined as the events of colocalization of ER tubule protrusion (detected with YFP-ER or GFP-STIM1) with EB3 comets or with growing MT plus ends. **E.** Number of sliding events, determined as the events of ER protrusion (detected with YFP-ER or GFP-STIM1), which did not colocalize with EB3 comets or with growing MT plus ends. Number of analysed cells: ER-MT: control, n = 20; EB1 #1, n = 20, EB1 #2, n = 15. ER-EB3: control, n = 20; STIM1 #1, n = 20, STIM1 #2, n = 20. STIM1-EB3: n = 20. STIM1-MT: control, n=10; EB1#1, n = 15, EB1 #2, n = 15. Values obtained in EB1 or STIM1 siRNA-treated cells that were significantly different from the corresponding values in cells treated with the control siRNAs are indicated by asterisks (p<0.001, ***; p<0.01, **; p<0.05, *; p>0.05, n.s., Kolmogorov-Smirnov test).